Manifold dimension of a causal set: Tests in conformally flat spacetimes

David D. Reid*
Department of Physics and Astronomy, Eastern Michigan University, Ypsilanti, Michigan 48197
(Received 23 July 2002; revised manuscript received 22 October 2002; published 30 January 2003)

This paper describes an approach that uses flat-spacetime estimators to estimate the manifold dimension of causal sets that can be faithfully embedded into curved spacetimes. The approach is invariant under coarse-graining and can be implemented independently of any specific curved spacetime. Results are given based on causal sets generated by random sprinklings into conformally flat spacetimes in 2, 3, and 4 dimensions, as well as one generated by a percolation dynamics.

DOI: 10.1103/PhysRevD.67.024034 PACS number(s): 04.60.−m, 04.20.Gz, 04.50.+h

I. INTRODUCTION

Since the time of Einstein, the prospect that spacetime might be discrete on microscopic scales has been considered as one possible avenue to help solve the problem of quantum gravity. The causal set program proposes one approach to discrete quantum gravity [1,2]. A causal set is a set C of elements $x_i \in C$, and an order relation $\prec$, such that the set $C=\{x_i,\prec\}$ obeys properties which make it a good discrete counterpart for continuum spacetime. These properties are that (a) the set is transitive: $x_i \prec x_j \prec x_k \Rightarrow x_i \prec x_k$; (b) it is noncircular, $x_i \prec x_j$ and $x_j \prec x_i \Rightarrow x_i = x_j$; (c) it is locally finite such that the number of elements between any two ordered elements $x_i \prec x_j$ is finite, i.e., $|[x_i,x_j]|<\infty$; and (d) it is reflexive, $x_i \prec x_i \ \forall x \in C$. The action of the order relation is to mimic the causal ordering of events in macroscopic spacetime. Since all events in spacetime are not causally related, then not all pairs of elements in the set are ordered by the order relation. Hence a causal set is a partially ordered set.

If the microscopic structure of spacetime is that of a causal set, then in appropriate macroscopic limits, causal sets must be consistent with the properties of general relativity which describes spacetime as a Lorentzian manifold. Therefore, it must be established that causal sets can possess manifold-like properties. A necessary (but not sufficient) requirement for a causal set to be like a manifold is that it can be embedded into a manifold uniformly with respect to the metric. Finding ways to embed a causal set has proven to be very difficult thus far. However, the properties of a causal set can be compared to the properties that a uniformly embedded causal set is expected to have. The kinds of tests that can check for manifold-like behavior generally require knowledge of the dimension of the manifold into which the causal set might embed. In fact, consistency between different ways to estimate the dimension of the manifold is itself a stringent test of manifold-like behavior. It is worth noting that within the mathematics of partial orders there are several types of dimensions. However, the dimensions traditionally studied by mathematicians do not correspond to what is meant here. Therefore, everywhere in this paper the phrase ''dimension of a causal set'' refers to the *manifold dimension*, i.e., the dimension of the Lorentzian manifold into which the causal set might be uniformly embedded.

The most useful methods for estimating the dimension of a causal set are the Myrheim-Meyer dimension [3,4] and the midpoint-scaling dimension [5]. By design, both of these methods work best in Minkowski space. The approach used to derive the Myrheim-Meyer dimension has been extended to curved spacetimes [4], but implementation of this more general *Hausdorff dimension* is specific to the particular spacetime against which the causal set is being checked. Since there are infinitely many curved spacetimes, this method is less useful in more generic cases. Therefore, there is a continuing need to find ways to estimate the dimension of a causal set for curved spacetimes that (a) are independent of the specific properties of the curved spacetime, (b) do not require very large causal sets to achieve useful results, and (c) are invariant under coarse-graining of the causal set. This last requirement is desired because, on the microscopic scale, the causal sets that might describe quantum gravity will not display manifold-like properties in the sense described above. Only in the macroscopic limit, after an appropriate change-of-scale, do we expect to see such properties; this change-of-scale is called coarse-graining.

In what follows, I first present the background theory and terminology needed to understand the dimension estimation methods described in this paper; then, the different approaches to dimension estimation are described. The extent to which the methods work is illustrated using causal sets generated by uniform sprinklings into flat and conformally flat spacetimes. I then illustrate the present method using a causal set generated by a percolation dynamics.

II. THEORY

As alluded to previously, in the causal set program we are interested in those causal sets that can be uniformly embedded into a manifold. An embedding of a causal set is a mapping of the set onto points in a Lorentzian manifold such that the lightcone structure of the manifold preserves the ordering of the set. With high probability, an embedding will be uniform if the mapping corresponds to selecting points in the manifold via a Poisson process (as described below). Two important results for understanding the dimension estimators to be discussed are (a) the correspondence between the volume of a region in a manifold and the number of causal set elements, and (b) the correspondence between geodesic

*Email address: phy_reid@online.emich.edu

length and the number of links in a chain of causal set elements. These topics are discussed in the next two subsections.

A. Random sprinklings

One way to generate a causal set that can be uniformly embedded into a manifold is to perform a random sprinkling of points in a manifold. If the set X consists of points $\{x_i\}$ randomly distributed (sprinkled) in a manifold M of finite volume V_M, we can define a discrete random variable χ_A on a region A of M such that $\chi_A(x_i)=1$ if $x_i \in A$ and 0 otherwise. In terms of the random variable χ_A we can define another discrete random variable N_n that counts the number of $x_i \in A$ up to a possible number n equal to the size of A, where $N_n=\Sigma_{i=1}^{i=n}\chi_A(x_i)$. Random variables such as N_n are described by the binomial distribution which, for our case, can be written as [4]

$$F_k(N_n)=\binom{n}{k}\left(\frac{V_A}{V_M}\right)^k\left(1-\frac{V_A}{V_M}\right)^{n-k}, \tag{1}$$

where F_k is the probability of outcome k.

If we define the density of the sprinkled points as $\rho=n/V_M$, the expectation value of N_n in region A is given by $\langle N_n\rangle=\rho V_A$. To generalize this description to manifolds of infinite volume, we take the limit of Eq. (1) as $V_M\to\infty$ while holding the density of the sprinkling uniform, $\rho=\text{const}$. This procedure is a standard approach for deriving the Poisson distribution [6]

$$P_k(N_n)=\lim_{\substack{V_M\to\infty\\ \rho=\text{const}}} F_k(N_n)=\frac{\rho V_A}{k!}e^{-\rho V_A}, \tag{2}$$

where the equivalence $V_A/V_M=\rho V_A/n$ has been used. From this distribution, we find that the average value of the number of points sprinkled into regions of volume V_A is given by

$$\langle N_n\rangle_A=\rho V_A. \tag{3}$$

While it is customary to scale the sprinkling to unit density, $\rho=1$, this scaling is not done in the present cases. Thus, we see that a random sprinkling of points in a manifold at uniform density is described by a Poisson distribution. Therefore, the interesting causal sets are from among those that will admit an embedding consistent with a Poisson sprinkling into a manifold (perhaps only after coarse-graining). Such an embedding is referred to as a *faithful embedding*.

B. Geodesic length

Recall that the length of the geodesic between two causally related events corresponds to the longest proper time between those events. To see what the most natural analog to geodesic length is for causal sets, we must first define a few terms. A *link*, $\preccurlyeq$, in a causal set is an irreducible relation; so, $x_i \preccurlyeq x_k$ iff $\nexists x_j \ni x_i \prec x_j \prec x_k$. A *chain* in a causal set is a set of elements for which each pair is related; for example, $x_a \prec x_b \prec \cdots \prec x_{z-1} \prec x_z$ is a chain from x_a to x_z. A *maximal chain* is a chain consisting only of links, such as $x_a \preccurlyeq x_b \preccurlyeq \cdots \preccurlyeq x_{z-1} \preccurlyeq x_z$.

As explained by Myrheim [3], the length of the longest maximal chain between two related elements in a causal set is the most natural analog for the geodesic length between two causally connected events in spacetime. (Myrheim did not use the term ''causal set'' which was coined by Rafael Sorkin and used in [1].) The length of a maximal chain is defined to be the number of links in that chain. Brightwell and co-workers have proven that this correspondence between the geodesic length in a Lorentzian manifold and the number of links in the longest maximal chain is, in fact, valid in Minkowski space [7]. Therefore, Myrheim's expectation that this correspondence should be valid in the general case seems well founded. In this work, I shall assume the validity of what I will refer to as the *Myrheim length conjecture*: Let $C=\{x_i,\prec\}$ be a causal set that can be faithfully embedded, with density ρ, into a Lorentzian manifold M by a map $g:C\to M$. Then, in the limit $\rho\to\infty$, the expected length of the longest maximal chain between any ordered pair $(x_i,x_j)\in C$ is directly proportional to the geodesic length between their images $[g(x_i),g(x_j)]\in M$.

III. DIMENSION ESTIMATORS

A dimension estimator for a causal set is a method that only uses properties of the set to determine the dimension of the manifold into which the causal set might be faithfully embeddable. Ideally, we hope to have a scheme for estimating the dimension of a causal set that (a) works well for curved spacetime manifolds, (b) is invariant under coarse-grainings of the causal set, and (c) does not require very large causal sets in order to see useful results. As alluded to previously, one difficulty in finding a useful dimension estimator for curved spacetimes is that implementation of the estimators tends to depend on the properties of the particular spacetime against which the causal set is being compared. This circumstance is problematic for causal sets generated by a process that does not directly suggest a class of candidate spacetimes.

However, one property that all physical spacetimes share is that locally, they are approximately Minkowskian. From the standpoint of causal sets, this implies that if a causal set C, of size N, is faithfully embeddable into a d-dimensional curved manifold M^d, then there ought to be subsets $c_i \subset C$, of size $n_i<N$ that are faithfully embeddable (approximately) into d-dimensional Minkowski space $\mathbb{M}^d$. Studying how these subsets behave under dimension estimators that work reliably for $\mathbb{M}^d$ should allow us to identify which, if any, d-dimensional Minkowski space is most closely approximated by these subsets. I will refer to dimensions found in the above manner as the *local Minkowski dimension* of the causal set. An approach similar to this was independently suggested by Sorkin [8].

The dimension estimators that will be used to determine the local Minkowski dimension in curved spacetimes are the Myrheim-Meyer dimension and the midpoint-scaling dimension mentioned in the Introduction and described below.

Both of these dimension estimators are defined in terms of causal set intervals. A causal set interval between two related elements $I[y,z]$ is the inclusive subset $I[y,z]=\{x_i|y\prec x_i \prec z\}$. Taking $\prec$ as a causal order, $I[y,z]$ is the intersection of the future of y with the past of z.

The Myrheim-Meyer dimension is based on the fact that for a causal set faithfully embeddable into an interval I of $\mathbb{M}^d$, the expected number of chains that consists of k elements, k-chains (S_k), is given by [4]

$$\langle S_k\rangle = \frac{(\rho V_I)^k \Gamma(\delta)\Gamma(2\delta)\Gamma(2\delta+1)^{k-1}}{2^{k-1}k\Gamma(k\delta)\Gamma((k+1)\delta)}, \tag{4}$$

where $\delta\equiv(d+1)/2$. The easiest chains to count are 2-chains which count the relations between elements. Specializing to 2-chains, Eq. (4) becomes

$$f(d)\equiv\frac{\langle S_2\rangle}{\langle N\rangle^2}=\frac{\Gamma(d+1)\Gamma(d/2)}{4\Gamma(3d/2)}, \tag{5}$$

where I have used Eq. (3) to relate number and volume. Therefore, for a given causal set, we can divide the number of relations $S_2\approx\langle S_2\rangle$ by the square of the number of elements $N\approx\langle N\rangle$ to approximate the value of $f(d)$ for the interval. This function is monotonically decreasing with d and can be numerically inverted to give a value for the dimension.

The midpoint-scaling dimension relies on the correspondence between number and volume, and on the relationship between the volume of an interval in $\mathbb{M}^d$ and the length of the geodesic τ between its defining events [5],

$$V_I=\frac{\pi^{(d-1)/2}}{2^{d-2}d(d-1)\Gamma[(d-1)/2]}\tau^d. \tag{6}$$

An interval $I[y,z]$ of size N can be divided into two subintervals $I_1[y,x]$ and $I_2[x,z]$ of sizes N_1 and N_2, respectively. Let N_{small} be the smaller of N_1 and N_2, then the element x is the midpoint of I when N_{small} is as large as possible. This process corresponds to a rescaling of lengths by a factor of 1/2; therefore, in the manifold $\tau/\tau_{small}=2$, which implies that $V/V_{small}=2^d$. For the causal set interval, assuming the Myrheim length conjecture, this translates to $N/N_{small}\approx 2^d$ so that

$$d\approx\log_2(N/N_{small}) \tag{7}$$

estimates the dimension.

IV. RESULTS

The dimension estimators were applied to causal set intervals generated by random sprinklings into flat and conformally flat spacetimes given by the metric

$$ds^2=\Omega^2\eta_{\alpha\beta}dx^\alpha dx^\beta, \tag{8}$$

where Ω^2 is the conformal factor (a smooth, strictly positive function of the spacetime coordinates) and $\eta_{\alpha\beta}$ is the Minkowski tensor. The sprinklings were performed by two different methods. The more efficient approach for sprinkling N points into an interval I of volume V was to divide the interval into several little regions of volume v_i. The number of points sprinkled into a region n_i was determined by the ratio $n_i/N=v_i/V$. The coordinates for the n_i points were then determined randomly within the region of volume v_i. The less efficient approach, which was much easier to implement, used a (double) rejection method similiar to the method described in [9]. In this second approach, the interval was enclosed in a box and spacetime coordinates were randomly selected within this box; if the selected point was outside the interval it was rejected, otherwise, it was kept—this was the first rejection. In Minkowski space, this first rejection provides a uniform distribution of points.

In curved spacetimes, points that fell within the interval faced a second rejection designed to ensure that the points were distributed uniformly with respect to the volume form Ω^d. Each point in the interval was associated with a random number w selected within the range $0<w<\Omega^d_{\max}$, where $\Omega^d_{\max}$ is the maximum value of the volume form within the interval I. If w was greater than the value of the volume form evaluated at the point in question, the point was rejected; otherwise, it was kept. This process continued until N points were sprinkled into the interval. The sprinklings in $1+1$ dimensions used the first method; all others used the rejection method. In a few cases the two methods were compared, and produced completely consistent results. That these methods produced causal sets that correspond to Poisson sprinklings was verified, in $1+1$ dimensions, by chi-squared tests. In all sprinklings, random numbers were generated using the subroutine ''ran2'' from [9].

Since the main result of this work comes from comparing the behavior of small sub-intervals between flat and curved spacetimes, we must determine the pertinent range of subinterval sizes. This range can be determined from sprinklings into Minkowski space. Figure 1 shows the results for random sprinklings of points into intervals of 2-, 3-, and 4-dimensional Minkowski space. Both the Myrheim-Meyer (d_{MM}) and midpoint-scaling (d_{mid}) dimensions were calculated for every closed sub-interval of size $n_i\geqslant 3$. The average value of d was calculated for sub-intervals of a given size. To decrease the statistical fluctuations, each curve in the figure represents an average of 15 different sprinklings.

While there are a number of interesting features in this figure, two things are most relevant to this study. First, we can see that for the midpoint-scaling dimension the three different Minkowski spaces are effectively indistinguishable for sub-intervals smaller than $n_i=10$. Therefore, since all three Minkowski results agree within this size region, any curved spacetime that behaves like one of these three should also be in agreement in this region. This fact sets the lower limit for the pertinent range of comparison with curved spacetimes at $n_i=3$. Second, the general trends displayed by these curves are typical for all of the results. The curves for both d_{MM} and d_{mid} rise steeply producing a ''shoulder'' beyond which the curves level off. The locations of the shoulder are clearly different for the three different spacetimes; therefore, the degree to which the analogous results for the

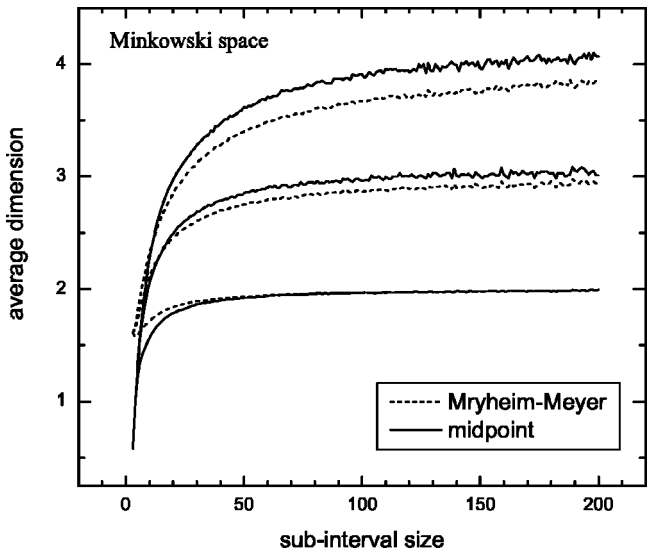

FIG. 1. The average value of the Myrheim-Meyer and midpoint dimensions for sub-intervals of a given size in $(1+1)$-, $(2+1)$-, and $(3+1)$-dimensional Minkowski space. The sprinklings in $1+1$ and $2+1$ dimensions are of 512 points, while, for better statistics, the $3+1$ sprinklings were of 1024 points. Each curve is an average of 15 different sprinklings. To clearly see the behavior of the small sub-intervals, results for sub-intervals containing only $n_i \leqslant 200$ are shown here. For $n_i > 200$ the results for the Myrheim-Meyer and midpoint dimensions, for the $2+1$ and $3+1$ sprinklings, also merge to the appropriate interger values.

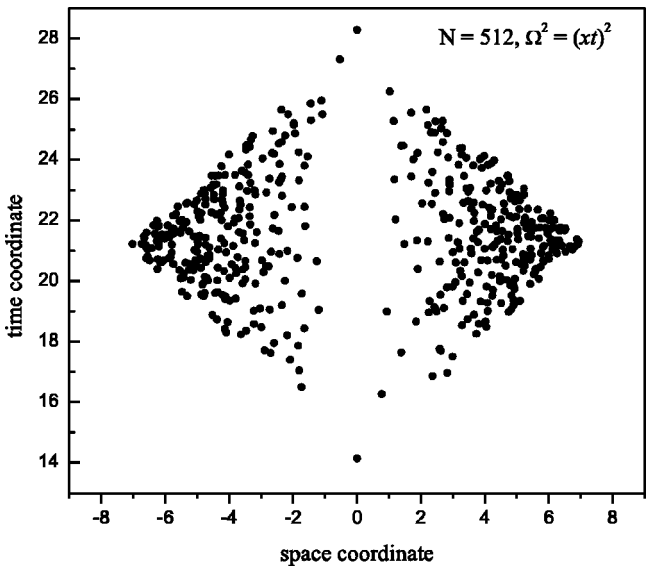

FIG. 2. A uniform sprinkling of 512 points into an interval of a conformally flat spacetime in $1+1$ dimensions. The conformal factor is shown in the figure.

curved spacetimes match these flat-spacetime results around this shoulder will be used to determine the local Minkowski dimension. The broadest shoulder occurs for $d=4$ for which a value of $n_i=100$ is sufficient to incorporate. Therefore, a good size range for seeking local Minkowski behavior for the curved spacetimes studied here is $3 \leqslant n_i \leqslant 100$. I will call this size range the *local Minkowski region*.

The quantitative measure of how well the results for a curved spacetime match those of a particular flat spacetime is a relative goodness-of-fit test using a chi-squared statistic that compares values of d for sub-intervals of the same size within the local Minkowski region. This relative measure requires knowledge of how well the different flat-spacetime results fit each other according to this method. The statistic is calculated as

$$\chi^2_{a,b} = \frac{1}{B} \sum_{j=1}^{B} \frac{(O_{ja} - E_{jb})^2}{E_{jb}}, \tag{9}$$

where the subscript (a,b) means that a-dimensional Minkowski space is being compared against b-dimensional Minkowski space. The quantity B is the number of bins into which the data were divided (either 22 or 30); this number depends on the bin size (either 4 or 3) which was chosen such that each ''expected'' value E_{jb} was greater than 5. The O_{ja} are the ''observed'' values. The results of these calculations for the Myrheim-Meyer dimension are the following: $\chi^2_{2,3}=0.662$, $\chi^2_{3,2}=1.25$, $\chi^2_{2,4}=1.77$, $\chi^2_{4,2}=4.20$, $\chi^2_{3,4}=0.365$, and $\chi^2_{4,3}=0.457$. For the midpoint dimension we also have the following results: $\chi^2_{2,3}=0.823$, $\chi^2_{3,2}=1.62$, $\chi^2_{2,4}=2.19$, $\chi^2_{4,2}=5.51$, $\chi^2_{3,4}=0.459$, and $\chi^2_{4,3}=0.588$. For both dimension estimators, the best (smallest) result comes from the comparison of three-dimensional Minkowski space against 4-dimensional Minkowski space. Therefore, these values will be used to determine the relative goodness-of-fit of the results for curved spacetimes, 0.365 for the Myrheim-Meyer calculations and 0.459 for the midpoint calculations.

A. 1+1 dimensions

Figure 2 shows a uniform sprinkling of 512 points into an interval of a conformally flat spacetime in $1+1$ dimensions with conformal factor $\Omega^2=(xt)^2$. Both the midpoint and Myrheim-Meyer dimension estimators fail for the full interval giving values of 2.77 and 2.65, respectively. The conformal factor for this spacetime causes the points to be more spread out in space which is consistent with the overestimates of the dimension. Figure 3 shows a plot of the average midpoint dimension for sub-intervals of different size averaged over 15 sprinklings of the spacetime shown in Fig. 2. This curve is compared against the results for Minkowski space. Despite the fact that the full interval values of the dimension estimators are closer to 3, the behavior for small sub-intervals clearly follows that of two-dimensional Minkowki space suggesting a local Minkowski dimension of 2. What appears to be happening here is that the small sub-intervals are, in fact, behaving like causal sets that are embeddable in two-dimensional Minkowski space; then, as you look at sub-intervals of larger size the effects of curvature become more important and the flat-spacetime dimension estimators become less reliable. (A similar plot using the Myrheim-Meyer dimension shows identical features.)

To quantify this result, a goodness-of-fit test is made, using an equation very similar to Eq. (9), which compares the average dimension of sub-intervals in the curved spacetime

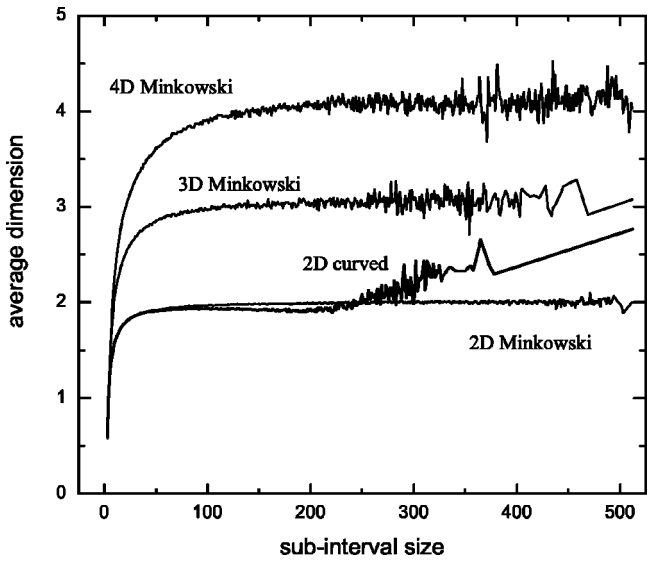

FIG. 3. Comparison of the average value of the midpoint-scaling dimension for sub-intervals of a given size for the set of points shown in Fig. 2 (2D curved) against the similar results for 2-, 3-, and 4-dimensional Minkowski space. The results for small sub-intervals suggest a local Minkowski dimension of 2.

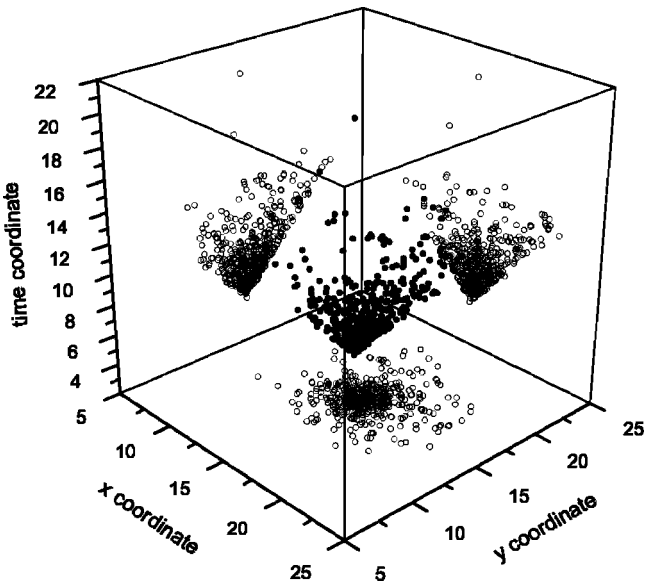

FIG. 4. A uniform sprinkling of 512 points into an interval of a conformally flat spacetime in $2+1$ dimensions with conformal factor $\Omega^2=(x^4+y^4)/t^6$. The figure also shows projections of the points onto the x-t, y-t, and x-y planes.

with those in each dimension of Minkowski space within the local Minkowski region. The curved spacetime values are taken as the observed and Minkowski space values as the expected. These results are then compared to the best chi-squared results from the mutual comparisons of the different dimensions of Minkowski space. For the curved spacetime shown in Fig. 2, we obtain relative goodness-of-fit values $\tilde{\chi}^2 \equiv \chi^2/\chi^2_{3,4}$ of

$$\tilde{\chi}^2_{2D,MM}=0.00181, \quad \tilde{\chi}^2_{2D,mid}=0.00119,$$

$$\tilde{\chi}^2_{3D,MM}=1.88, \quad \tilde{\chi}^2_{3D,mid}=1.84, \tag{10}$$

$$\tilde{\chi}^2_{4D,MM}=4.95, \quad \tilde{\chi}^2_{4D,mid}=4.84,$$

where the notation $\tilde{\chi}^2_{2D,MM}$ means that the curved spacetime result was compared against two-dimensional Minkowski space using the average Myrheim-Meyer dimension values relative to the value of $\chi^2_{3,4}$ for the Myrheim-Meyer dimension; and correspondingly for the values labeled with the subscript ''mid.'' As defined, this statistic means that values of $\tilde{\chi}^2 \gtrsim 1$ represent a poor fit signifying that the two data sets being compared could certainly be Minkowski spaces differing in dimension by at least 1, whereas values of $\tilde{\chi}^2 \ll 1$ indicate a good fit with the spacetime in question. Clearly, the results displayed in Eq. (10) show that the small sub-intervals offer an excellent fit to those of two-dimensional Minkowski space. Furthermore, the fits with three- and four-dimensional Minkowski space are no better, or much worse, than what can be expected between Minkowski spaces of different dimensions. The conformally flat spacetime for which the above results are given represents only one of several $(1+1)$-dimensional spacetimes studied. In all cases, the results are similiar to those given here.

B. 2+1 dimensions

Figure 4 shows a uniform sprinkling of 512 points into an interval of a conformally flat spacetime in $2+1$ dimensions with conformal factor $\Omega^2=(x^2+y^2)/t^6$. This example was chosen because it produced the worst full interval results for all of the $(2+1)$-dimensional spacetimes studied. It is easier to see what this interval is like from the projections. The y-t plane shows that more points are located at larger values of the y coordinate and smaller values of t; the x-t plane shows similar behavior. The projection onto the x-y plane shows that the points are more crowded in the middle of the interval. This crowding is due to the preference for small t where the spatial extent of the region is centralized.

Figure 5 shows a plot of the average Myrheim-Meyer dimension for sub-intervals of different size averaged over 15 sprinklings of the spacetime shown in Fig. 4. This curve is compared against the results for Minkowski space. For this spacetime, the effects of the curvature become apparent around $n_i=40$. Nevertheless, the result for the curved spacetime maintains a good approximation to the flat spacetime result within the designated locally flat region. To verify that the local Minkowski dimension of this spacetime should be taken to be 3, the relative goodness-of-fit results are

$$\tilde{\chi}^2_{2D,MM}=3.03, \quad \tilde{\chi}^2_{2D,mid}=3.15,$$

$$\tilde{\chi}^2_{3D,MM}=0.00807, \quad \tilde{\chi}^2_{3D,mid}=0.00697, \tag{11}$$

$$\tilde{\chi}^2_{4D,MM}=1.15, \quad \tilde{\chi}^2_{4D,mid}=1.14.$$

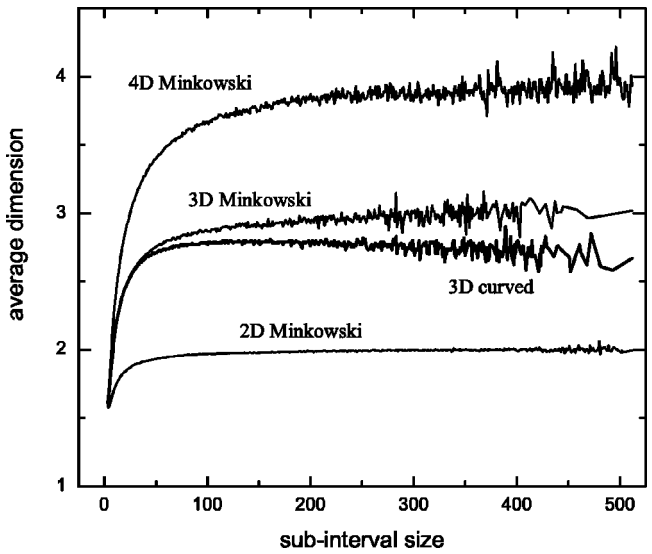

FIG. 5. Comparison of the average value of the Myrheim-Meyer dimension for sub-intervals of the set shown in Fig. 4 (3D curved) against similar results for Minkowski space. The results for small sub-intervals suggest a local Minkowski dimension of 3.

Here we see clearly that in the locally flat region this spacetime provides results that give an excellent fit to the results for three-dimensional Minkowski space. Several other spacetimes in $2+1$ dimensions were studied giving similar results.

C. 3+1 dimensions

Figure 6 shows projections of a uniform sprinkling of 512 points into an interval of a conformally flat spacetime in $3+1$ dimensions with conformal factor $\Omega^2=(x^4+y^4+z^4)/t^6$. Figure 7 is the corresponding plot for the average

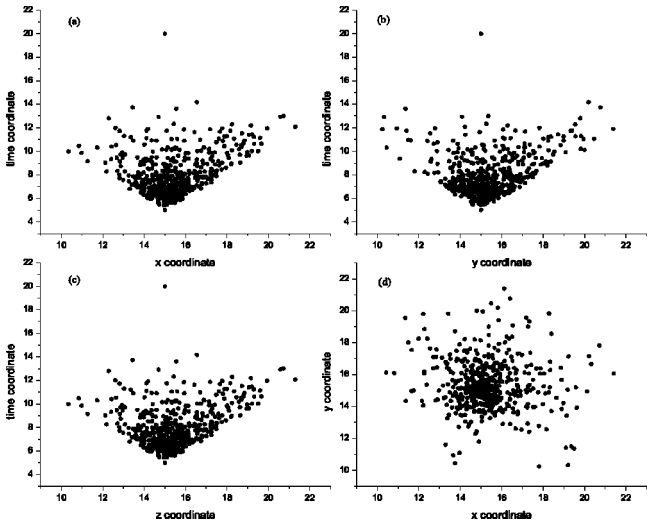

FIG. 6. Projections of a uniform sprinkling of 512 points into an interval of a conformally flat spacetime in $3+1$ dimensions with conformal factor $\Omega^2=(x^4+y^4+z^4)/t^6$. Panel (a) shows the projection onto the x-t plane, panel (b) shows the projection onto the y-t plane, panel (c) shows the projection onto the z-t plane, and panel (d) shows the projection onto the x-y plane.

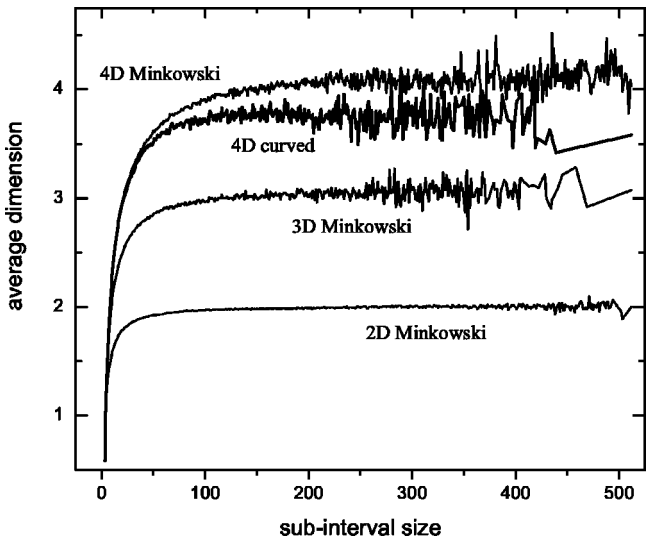

FIG. 7. Comparison of the average value of the midpoint-scaling dimension for sub-intervals of the set represented in Fig. 6 (4D curved) against similar results for Minkowski space. The results for small sub-intervals suggest a local Minkowski dimension of 4.

dimension per size of the sub-interval. As with the other cases, the figure clearly shows that within the locally flat region the curved spacetime result gives a much better fit to the Minkowski space having the same dimension. The relative goodness-of-fit results for this case are

$$\tilde{\chi}^2_{2D,MM}=9.62,\quad \tilde{\chi}^2_{2D,mid}=10.4,$$

$$\tilde{\chi}^2_{3D,MM}=0.825,\quad \tilde{\chi}^2_{3D,mid}=0.919, \tag{12}$$

$$\tilde{\chi}^2_{4D,MM}=0.0382,\quad \tilde{\chi}^2_{4D,mid}=0.0252.$$

Several other spacetimes in $3+1$ dimensions were studied giving similar results.

D. A causal set generated by transitive percolation

So far, all of the causal sets used were guaranteed to be faithful because they were generated by sprinklings into known manifolds. Having established the approach, it is instructive to apply this method to a causal set generated by some other means. Ultimately, there will be a quantum dynamics for generating causal sets, and it will be these causal sets (or coarse-grained versions of them) whose manifold dimensions we would like to estimate. Although a quantum dynamics for causal sets does not yet exist, there is a classical dynamics, due to Rideout and Sorkin [10], which is proving to be very useful in helping to determine the extent to which causal sets can encode physical information. So, this classical dynamics provides an excellent avenue to illustrate how the suggestions presented here might be used in a more general case when we cannot be sure that the causal set is faithfully embeddable.

Perhaps the simplest model within the class of models proposed by Rideout and Sorkin is the one that they have

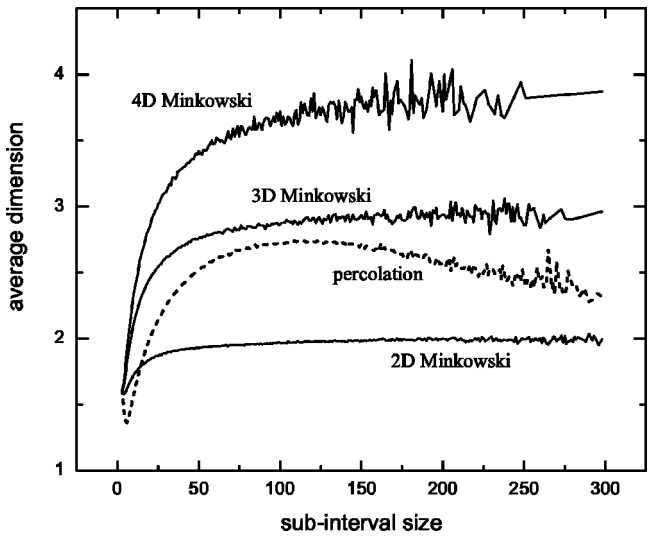

FIG. 8. Comparison of the average value of the Myrheim-Meyer dimension for the largest sub-interval of a 512-element causal set generated by transitive percolation. The results for small sub-intervals do not match any of the three Minkowski space results suggesting that this percolated causal set is not faithfully embeddable into any spacetime manifold.

called transitive percolation. The procedure followed here for generating a random causal set of N elements via percolation is as follows: (a) assign labels to the N elements; (b) impose the partial ordering relation $\prec$ onto each pair of elements with probability p, that is, if $i<k$, the probability that element $i<$element k is p; and (c) enforce the transitivity requirement on the set. It has been shown that despite the labeling, causal sets generated in this way are label invariant in that the probability of getting a particular causal set is independent of how the elements were initially labeled [10].

For this example, a causal set with $N=512$ and $p=0.0261$ was generated; these values produce a causal set that has a Myrheim-Meyer dimension of 2.0 when applied to the full causal set [11]. This causal set, however, is not a causal set interval. Therefore, the largest sub-interval of this 512-element causal set was used; this sub-interval contained 298 elements. Figure 8 is a plot of the average Myrheim-Meyer dimensions for the sub-intervals of the 298-element causal set interval taken from the causal set generated by transitive percolation, compared against 298-element causal sets generated by random sprinklings in Minkowski space. What stands out in this figure is that the percolation curve does not closely follow any of the Minkowski curves in the local Minkowski region. Therefore, not even the small sub-intervals of this causal set behave as sub-intervals in Minkowski space do. This suggests that the percolated causal set should not be embeddable into any (flat or curved) spacetime.

Looking at Fig. 8 shows that the percolation curve is a closer fit to the three-dimensional Minkowski curve than it is to the other curves. The relative goodness-of-fit test yields

$$\tilde{\chi}^2_{2D,MM}=1.82, \quad \tilde{\chi}^2_{3D,MM}=0.308, \quad \tilde{\chi}^2_{4D,MM}=1.952. \tag{13}$$

While these results confirm that the percolation curve is a better fit to the three-dimensional Minkowski result, we can also see that the $\tilde{\chi}^2_{3D}$ value is nearly two orders-of-magnitude worse than what would be expected based on our study of the random sprinklings. This fact gives some quantitative weight to the conclusion reached by studying Fig. 8.

V. CONCLUSIONS

In this paper, I have suggested a method for estimating the manifold dimension of a causal set that can be faithfully embedded into curved spacetimes and tested this method for several conformally flat spacetimes. The method uses flat-spacetime dimension estimators to search for local Minkowski behavior within the causal set. This approach can be applied to any causal set, and works independent of the specific properties of a particular curved spacetime. Very large causal sets are not required. Furthermore, this approach is invariant under coarse-graining since both the Myrheim-Meyer and midpoint-scaling dimensions are invariant under coarse-graining.

Implementation of this procedure can be summarized as follows: (a) form an interval of size N of the causal set, larger intervals give better statistics, but they do not need to be extremely large; (b) average the Myrheim-Meyer (or midpoint-scaling) dimension for sub-intervals of a given size; (c) perform ramdom sprinklings of size N or greater in 2-, 3-, and 4-dimensional Minkowski space and determine average dimension values for their sub-intervals; (d) a comparision of the results for the causal set being checked against the results for the three Minkowski sprinklings for small sub-intervals, $3<n_i<100$, should reveal whether or not the causal set in question displays the local Minkowski behavior that would be required of causal sets that are faithfully embeddable into physically relevant spacetimes.

It is worth noting that instead of calculating the dimension values for closed sub-intervals, open sub-intervals can also be used. However, the statistical fluctuations are greater for open sub-intervals and this fact becomes somewhat problematic in $2+1$ and especially in $3+1$ dimensions. What now remains is to apply this method to generically curved spacetimes. The basic principle behind the local Minkowski dimension certainly applies in the generic case, but the extent to which this behavior can be extracted from the causal sets is yet unknown. If this approach proves useful in that case as well, it would be an important step toward the goal of a more comprehensive manifold test for causal sets.

ACKNOWLEDGMENTS

I would like to acknowledge Jason Ruiz for writing the computer code to conduct the chi-squared tests used to test the faithfulness of some of the sprinklings. I also wish to thank Dr. Rafael D. Sorkin for providing information on the percolation dynamics and further motivation to work on problems in causal set quantum gravity. This work benefited from the research support programs of Eastern Michigan University. Additional support from the National Science Foundation is gratefully acknowledged.

[1] L. Bombelli, J. Lee, D. Meyer, and R.D. Sorkin, Phys. Rev. Lett. **59**, 521 (1987); **60**, 656 (1988).
[2] D.D. Reid, Can. J. Phys. **79**, 1 (2001).
[3] J. Myrheim, CERN Report No. TH-2538 (1978).
[4] D. Meyer, Ph.D. thesis, M.I.T., 1988.
[5] L. Bombelli, Ph.D. thesis, Syracuse University, 1987.
[6] M.H. DeGroot, *Probability and Statistics* (Addison-Wesley, Reading, 1975).
[7] G. Brightwell and R. Gregory, Phys. Rev. Lett. **66**, 260 (1991).
[8] R.D. Sorkin, in *General Relativity and Gravitational Physics. Proceedings of the Ninth Italian Conference on General Relativity and Gravitational Physics, 1990*, edited by R. Cianci, R. de Ritis, M. Francaviglia, G. Marmo, C. Rubano, and P. Scudellaro (World Scientific, Singapore, 1991), pp. 68–90.
[9] W.H. Press, S.A. Teukolsky, W.T. Vetterling, and B.P. Flannery, *Numerical Recipes in Fortran: The Art of Scientific Computing*, 2nd ed. (Cambridge University Press, Cambridge, England, 1992).
[10] D.P. Rideout and R.D. Sorkin, Phys. Rev. D **61**, 024002 (2000).
[11] R.D. Sorkin (private communication).